Astron. Astrophys. 315, L381–L384 (1996)

ASTRONOMY
AND
ASTROPHYSICS

Mid-Infrared spectrum of the zodiacal light⋆

W.T. Reach[1], A. Abergel[1], F. Boulanger[1], F.-X. Désert[1], M. Perault[4], J.-P. Bernard[1], J. Blommaert[3], C. Cesarsky[2], D. Cesarsky[1], L. Metcalfe[3], J.-L. Puget[1], F. Sibille[5], and L. Vigroux[2]

[1] Institut d'Astrophysique Spatiale, Bât. 121, Université Paris XI, F-91405 Orsay Cedex, France
[2] Service d'Astrophysique, Centre d'Etudes de Saclay, F-91191 Gif-sur-Yvette Cedex, France
[3] ISO Science Operations Centre, Astrophysics Division of ESA, Villafranca, Spain
[4] Ecole Normale Supérieure, Paris, France
[5] Observatoire de Lyon, Lyon, France

Received 16 July 1996 / Accepted 23 August 1996

Abstract. Using the mid-infrared camera on the *Infrared Space Observatory* (*ISO*), the spectrum of a relatively empty piece of sky, dominated by zodiacal light, was measured from 5 to 16.5 μm wavelength. The spectrum has no spectral features brighter than 15% of a blackbody fit to entire spectrum; the temperature of the fit is 261.5 ± 1.5 K. No galactic or cosmic background spectral features are detected. Comparison to models for three size distributions of spherical grains composed of several different materials reveals acceptable fits only for 'astronomical silicate,' ruling out graphite, magnetite, andesite, obsidian, glassy carbon, or water ice as the constituent of material producing the zodiacal emission. The size distribution is constrained to have relatively fewer small particles compared to the coma of P/Halley. There is a hint of a 9–11 μm feature, which suggests that the particles producing the zodiacal light are composed of silicates similar to those found in the coma of P/Halley, collected interplanetary dust particles, and the dust around the nearby star β Pic.

Key words: interplanetary dust – background radiation – zodiacal light

1. Introduction

Solid particles permeate the interplanetary medium and produce such diverse phenomena as meteors, comet tails, microcraters on lunar rocks, penetration of satellite detectors and shields, sea-floor and arctic ice micrometeorites, and stratospheric dust (Brownlee 1985). Each phenomenon is produced by a different range of particle sizes in a different set of trajectories. Particles larger than $\sim$ 1 μm, heated by the Sun to temperatures $\sim$ 300 K, cool through thermal emission at mid-infrared wavelengths. Nearly all previous space-based observations of this zodiacal emission – such as those by *COBE*/DIRBE (Boggess et al. 1992) – have been broad-band photometry. Spectral observations with even moderate resolution provide a significantly different view of the zodiacal light that can be compared to laboratory measurements both of candidate materials and of collected stratospheric particles and meteorites. In the near-infrared (1.4–2.5 μm), where the zodiacal light is dominated by scattering, the spectrum observed in rocket experiments was found to be featureless but redder than the incident sunlight (Matsuura et al. 1995). The spectrum of the thermal emission was only measured in an early rocket experiment, from which a silicate emission line was reported (Briotta 1976).

With the launch of the *Infrared Space Observatory* (*ISO*, Kessler et al. 1996), several new and powerful instruments are all observing the zodiacal light. The observations reported here, with the mid-infrared camera (ISOCAM, Cesarsky et al. 1996) cover the spectral region 5–16 μm. Interplanetary particles collected from the stratosphere have been shown to absorb in the 9–11 μm silicate band (Sandford & Walker 1985), for which the present observations are well designed. Furthermore, cometary (Hanner et al. 1994) and circumstellar (Knacke 1993) have structured silicate bands, and we hope to compare the dust that produces the zodiacal light to its origin as well as to dust around other stars.

The zodiacal light is the dominant contribution to the diffuse sky brightness throughout most of the infrared spectrum. The presence of such a strong foreground limits the sensitivity of most space experiments for detecting extended sources, in particular the diffuse emission from outside the Solar System (Hauser 1996).

Send offprint requests to: W.T. Reach, reach@ias.fr

⋆ Based on observations with the Infrared Space Observatory (ISO). ISO is an ESA project with instruments funded by ESA Member States (especially the PI countries: France, Germany, the Netherlands and the United Kingdom) and with the participation of ISAS and NASA.

2. Observations

Several patches of sky, selected for their isolation from any diffuse, structured emission on the *IRAS* 12 μm images and free of any bright stars, were observed during the performance verification phase of the *ISO* mission. A complete scan of the long-wavelength ISOCAM circular variable filters (CVF) was performed toward ecliptic longitude $196\overset{\circ}{.}6$ and latitude $-2\overset{\circ}{.}4$, (13^h right ascension, -9° declination, J2000) on 21 Jan 1996, at a solar elongation of $104\overset{\circ}{.}3$. The 6" pixel-field-of-view lens was used. First, the LW-CVF2 was rotated such that the wavelength varied from 16.5 to 9.0 μm, then the LW-CVF1 was rotated such that the wavelength varied from 9.4 to 5.0 μm ('*aller*'). Then, the same process was reversed ('*retour*'). At each step of the CVF, 15 frames of 2.1 sec were taken. After the CVF spectrum, we added two long stares at the same position, one in the LW8 (11.4 μm) filter and the other at a fixed position (11.27 μm) of the LW-CVF2, as a test on the stability of the photometry. The entire process lasted about 3 hr.

The complete set of 4884 raw images was temporally filtered to remove cosmic ray events (some 4% of the data). The mean over the central 12 pixels of each image was calculated and coadded for each wavelength, and the mean dark current over the same pixels was subtracted. The observed brightness at the shortest wavelength was only about 2 ADU above the dark level, Because the measured dark current varied somewhat during the performance-verification phase of the mission, we consider the dark level accurate to $\sim \pm 0.3$ ADU (1-σ). The dark current is the dominant uncertainty at wavelengths below 8 μm.

Another consequence of the low light levels is that the detectors are very slow to stabilize. The stabilization timescale for the observation presented here is estimated to range from 200 seconds (at 12 μm) to over an hour (at 5 μm). We used an experimental algorithm that corrects for the gain drift using the integrated brightness over the previous images. Before transient corrections, the '*retour*' spectrum was some 13% fainter at 10 μm, because the stabilization timescale is very low when the illumination increases from very low levels. After correction, the agreement is good, and we use the absolute difference between the two spectra to estimate the systematic gain error. The stability of the photometry was checked by comparing to the two staring observations in a single position of the CVF and in the LW8 filter, as shown in Fig. 1.

The spectral response of the detectors was calibrated using the ratio of observed to model (Kurucz 1979) spectrum of HD 185395, an F-type main-sequence star. The model has been scaled to match ground-based photometry, as part of the *ISO* Ground-Based Preparatory Program (courtesy P. Hammersley). The resulting spectral response contains variations at the $\sim 15\%$ level relative to the pre-flight calibration. Nearly the same result was obtained by comparing ISOCAM and ground-based spectra for a K giant star. This same spectral response was used to calibrate ISOCAM CVF spectra of a diverse range of astronomical targets and found not to introduce spurious features. The observed spectrum of the star becomes noisy at the longer wavelengths, and this increases the noise in the calibrated spectrum.

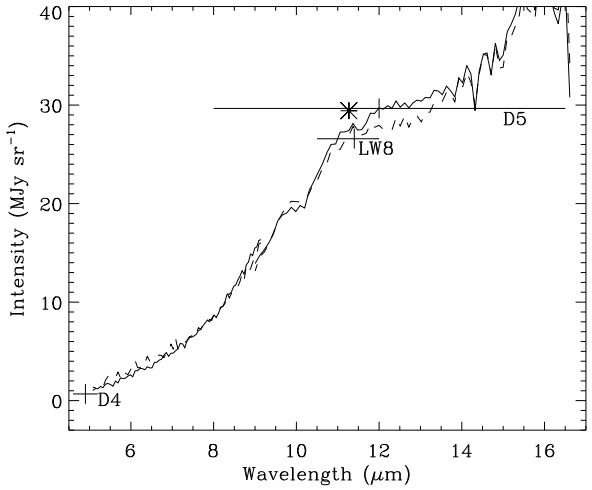

Fig. 1. Spectrum of an empty, high-galactic-latitude field with the ISOCAM CVF. Two spectra were obtained with wavelength decreasing with time ('*aller*,' solid curve) and wavelength increasing with time ('*retour*,' dashed curve). Around 9 μm, the spectra from the two sections of the CVF overlap. Two long staring observations at the 11.27 μm position of the CVF and in the LW8 filter are shown as an asterisk and horizontal line, respectively. The brightnesses observed by DIRBE in the 4.9 and 12 μm wavebands are shown as long horizontal lines labelled 'D4' and 'D5', respectively. The length of each line represent the FWHM of the DIRBE band.

3. Results

The calibrated spectrum of the zodiacal light is shown in Figure 1. The spectrum contains no obvious spectral features, and it is close to that of a blackbody at a temperature of 261.5 ± 1.5 K (best fit and 1-σ uncertainty). The ratio of the observed spectrum to the blackbody function is shown in Figure 2. The uncertainties are generally correlated from wavelength to wavelength (especially that due to dark current), and therefore they overestimate the relative spectral uncertainty. The structure in the 9–11 μm range is potentially interesting but at present comparable to uncertainty due to transient gain response. The spectrum we obtained here is different from that obtained in a pioneering rocket experiment (Briotta 1976), from which a prominent silicate feature was inferred; the shortest-wavelength channels of the rocket spectrum may have been contaminated.

In order to check our absolute calibration, we compared to the average sky brightness in a 3° circle from the DIRBE weekly skymaps, interpolated to our observing date. The agreement between the ISOCAM and DIRBE observations is within the absolute calibration uncertainties of the two instruments. For a more complete assessment of the absolute photometry of ISOCAM, we compared several flat-field observations in various filters to the corresponding brightness interpolated from the DIRBE skymaps. The agreement between ISOCAM and

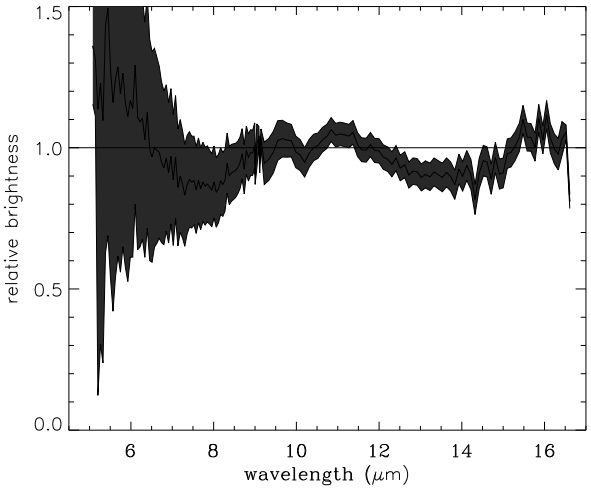

Fig. 2. Ratio between the zodiacal light spectrum and a blackbody at 261.5 K. The grey region is the $\pm 1\sigma$ band allowed by uncertainties in the dark current (dominating at short wavelengths) and the gain stability (dominating at longer wavelengths).

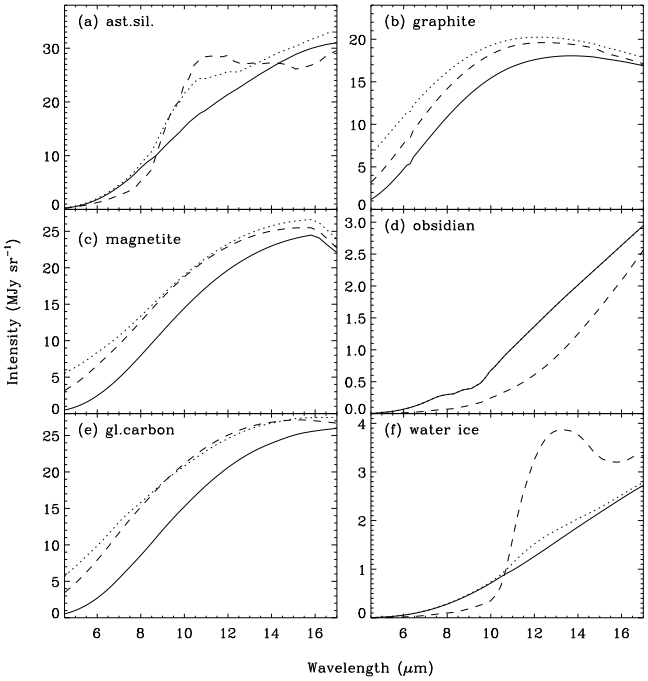

Fig. 3. A suite of models of the zodiacal light spectrum. Each panel corresponds to one constituent material: *(a)* astronomical silicate, *(b)* graphite, *(c)* magnetite, *(d)* obsidian, *(e)* glassy carbon, and *(f)* water ice. Within each panel, the three curves correspond to different size distributions; *solid*: interplanetary, *dotted*: lunar (Grün et al. 1985), and *dashed*: P/Halley (Lamy et al. 87). For each model, the emission from an ensemble of spherical particles, illuminated by the Sun, was integrated over the particle size distribution and line of sight. Comparison to the observed spectrum clearly rules out nearly all of the models shown here. The only models close to the observations are astronomical silicate with the interplanetary or lunar size distribution model (solid and dashed curves in panel *(a)*) or andesite with the lunar size distribution (dashed curve in panel *(b)*).

DIRBE photometry is good, demonstrating that ISOCAM can be used as a photometer.

4. Interpretation

4.1. Comparison to models

For comparison with the observations, we created a suite of models using the optical properties of 7 constituent materials and 3 different size distributions; the calculations are an update of previous ones (see Reach 1988 for details). The emission is dominated by dust within about 1 AU of the Earth; we have approximated the line-of-sight integral using a weighted combination of models at 1 AU and 1.5 AU from the Sun. Results are shown in Figure 3. Many of the models predict spectral features that are clearly not observed. Specifically, the silicate models ('astronomical silicate,' andesite, and obsidian) with abundant small particles (as in P/Halley) present very strong Si–O features at 9–11 μm. Water Ice also presents a strong line, at 13 μm, for two of the three size distributions.

We have evaluated the models for the same wavelength grid as the observations and calculated the χ^2 goodness-of-fit or each, using the uncertainties due to dark current and gain stability. The best-fitting constituent material is 'astronomical silicate' (Draine & Lee 1984), which results in a reduced $\chi^2 = 2.3$ with the 'interplanetary' and 2.1 with the 'lunar' size distributions (Grün et al. 1985). Andesite, which is similar to 'astronomical silicate' but with somewhat less visible absorption (Reach 1988), results in $\chi^2 = 2.7$ with the 'lunar' size distribution. The other models are ruled out at very high levels of confidence, as may be seen by comparing observed and model color ratios. The ratios of convolutions of the observed and model spectra with the ISOCAM LW6 (7.75 μm), LW7 (9.63 μm), and LW9 (15.0 μm) filters are shown in Table 1. Strongly absorbing materials (graphite, magnetite, glassy carbon) are much too hot and can be clearly ruled out by their high 7.75/15 ratios. Conversely, more transparent materials (obsidian, water ice) are too cold and are ruled out by low color ratios. In addition to the color ratios, the transparent materials produce far too little emission to explain the observed brightness level; conversely, we would not easily detect a population of such particles.

4.2. The silicate emission band

In order to measure the shape of the silicate feature of the zodiacal light, we estimated the continuum two ways: (1) using the blackbody fit to the entire observed spectrum, and (2) using the best-fitting model that does *not* produce a silicate line ('astronomical silicate' with the 'interplanetary' size distribution). In the first case the residual brightness is positive by about 10% in the 9–11 μm range, then negative by similar amounts on either side, with a rise again at short wavelengths (Fig 2). The models include some emission by smaller, hotter particles,

Table 1. Zodiacal light mid-infrared colors

	9.63 μm/15 μm			7.75 μm/15 μm		
material	IP	LU	HA	IP	LU	HA
AST.SIL.	0.46	0.57	0.67	0.22	0.22	0.15
GRAPHITE	0.77	0.81	0.89	0.51	0.59	0.67
MAGNETITE	0.53	0.63	0.67	0.27	0.40	0.44
ANDESITE	0.37	0.42	0.45	0.18	0.19	0.11
OBSIDIAN	0.25	0.42	0.13	0.11	0.13	0.04
GLASS CARB.	0.53	0.67	0.72	0.28	0.45	0.50
WATER ICE	0.29	0.43	0.14	0.11	0.13	0.03
Observed	0.51 ± 0.07			0.22 ± 0.05		

IP=interplanetary size distribution
LU=lunar size distribution
HA=P/Halley size distribution

as well as a spread of cooler temperatures along the line of sight, and are a better fit than the blackbody curve. Using the solid curve in Fig. 3*(a)* as a continuum, the residual brightness is positive in the 9–11 μm range but otherwise flat. Thus there is tentative evidence for a silicate feature in the zodiacal light. The shape of this residual feature is significantly different from those produced by small 'astronomical silicate' or andesite, which rise and decline at shorter wavelengths (by about 0.7 μm). The mid-infrared spectra of many comets have structured 9–11 μm emission bands fully 50% as bright as the continuum (Hanner et al. 1994), and the dust around the nearby star β Pic has a very similar line that is even brighter relative to the continuum (Knacke 1993). The shape of the zodiacal light silicate line is very similar to those of comet P/Halley and the circumstellar dust around β Pic, but the zodiacal light silicate line is superposed on a relatively brighter continuum. A confirmation of the silicate feature in the zodiacal light will require a more complete study, which is currently under way, understanding of the behavior of the ISOCAM detectors at low light levels. We further expect zodiacal light spectra to be obtained from reference fields of some other astronomical observations by ISOCAM, and we will be able to compare these independent results.

5. Conclusions

The zodiacal light spectrum from 5 to 16.5 μm obtained with ISOCAM provides strong constraints on the composition and size of interplanetary dust. The continuum can be approximated by a blackbody with a temperature of 261.5 ± 1.5 K, and it is reasonably well fit by particles with a size distribution such as measured in near-Earth orbit. There is some evidence of a 9–11 μm feature, indicating that the particles producing the zodiacal light are composed of silicates similar to those found in the coma of P/Halley, collected interplanetary dust particles, and the dust around the nearby star β Pic. Finally, we limit the brightness of any unresolved spectral lines in the infrared background to $< 5 \times 10^{-9}$ W m^{-2} sr^{-1} from 5.4 to 13 μm, or and $< 1.5 times 10^{-8}$ W m^{-2} sr^{-1} from 13 to 16.3 μm.

Acknowledgements. WTR thanks Jim Houck for providing and discussing the early rocket observations.

References

Boggess, N. W., Mather, J. C., Weiss, R., Bennett, C. L., Cheng, E. S., Dwek, E., Gulkis, S., Hauser, M. G., Janssen, M. A., Kelsall, T., Meyer, S. S., Moseley, S. H., Murdock, T. L., Shafer, R. A., Silverberg, R. F., Smoot, G. F., Wilkinson, D. T., E. L. Wright 1992, ApJ, 397, 420
Briotta, D. A., Jr. 1976, Ph. D. Thesis, Cornell Univ.
Brownlee, D. E. 1985, Ann. Rev. Earth Planet. Sci., 14, 147
Cesarsky, C. J. et al. 1996, A& A, this issue
Draine, B., Lee, H. 1984, ApJ, 285, 89
Grün, E., Zook, H. A., Fechtig, H., Giese, R. H. 1985, Icarus, 62, 244
Hanner, M. S., Lynch, D. K., Russell, R. W. 1994, ApJ, 425, 274
Hauser, M. G. 1996, in *Unveiling the Cosmic Infrared Background*, ed. E. Dwek (New York: AIP)
Kessler, M. et al. 1996, A& A, this issue
Knacke, R. F., Fajardo-Acosta, S. B., Telesco, C. M., Hackwell, J. A., Lynch, D. K., Russell, R. W. 1993, ApJ, 418, 440
Kurucz, R. L. 1979, ApJS, 40,1
Lamy, P. L., Grü n, E., Perrin, J. M. 1987, A& A, 187, 767
Matsuura, S., Matsumoto, T., Matsuhara, H., & Noda, M. 1995, Icarus, 115, 199
Reach, W. T. 1988, ApJ, 335, 468
Sandford, S., Walker, R. 1985, ApJ, 291, 838